

Article ID: 1007-7294(2025)06-0964-12

Investigation on the Ice Load on a Cylinder Vertically Breaking through Model Ice Sheet from Underneath

ZHAO Wei-hang, TIAN Yu-kui, JI Shao-peng, GANG Xu-hao, YU Chao-ge, KONG Shuai
(China Ship Scientific Research Center, Wuxi 214082, China)

Abstract: Ice load on underwater vehicles breaking through ice covers from underneath is a significant concern for researchers in polar exploration, and the research on this problem is still in its early stages. Both mechanical experimental measurement and numerical simulation pose research challenges. This study focuses on the ice load of a cylinder structure breaking upward through the ice sheet from underneath in the Small Ice Model Basin of China Ship Scientific Research Center (CSSRC SIMB). A high-speed camera system was employed to observe the ice sheet failure during the tests, in which, with the loading position as center, local radial cracks and circumferential cracks were generated. A load sensor was used to measure the overall ice load during this process. Meanwhile, a numerical model was developed using LS-DYNA for validation and comparison. With this model, numerical simulation was conducted under various ice thicknesses and upgoing speeds to analyze the instantaneous curves of ice load. The calculation results were statistically analyzed under different working conditions to determine the influence of the factors on the ice load of the cylinder. The study explores the measurement method about ice load of objects vertically breaking through model ice sheet and is expected to provide some fundamental insights into the safety design of underwater structures operating in ice waters.

Key words: cylinder; model test; failure mode; crack propagation; ice load; numerical modeling

CLC number: P75 P731.15 **Document code:** A **doi:** 10.3969/j.issn.1007-7294.2025.06.010

0 Introduction

The melting of Arctic sea ice has resulted in the opening of the Arctic route^[1]. However, navigating in the Arctic region has proved to be a challenge due to unexpected situations, with underwater vehicles stuck in ice being a relatively common emergency. In such events, vehicles often find it difficult to extricate themselves and require auxiliary ice-breaking methods. The focus of most of the existing research is placed on longitudinal and transverse ice-breaking^[2]. However, neither of these methods is suitable for solving the problem of an underwater vehicle stuck in ice. On the other side, some scholars think that vertical ice-breaking has demonstrated superior efficacy in dealing with underwater vehicles stuck in ice^[3]. During vertical ice-breaking, the ice sheet undergoes shearing and bending failures, which will assist vehicles in freeing themselves from the ice sheet. Furthermore, when designing offshore structures, it is essential to

Received date: 2024-12-21

Foundation item: Supported by the National Natural Science Foundation of China (52192694; 52192690) and Hi-Tech Ship Project of the Ministry of Industry and Information Technology ([2021]-342)

Biography: ZHAO Wei-hang(1998-), male, assistant engineer; TIAN Yu-kui(1968-), male, corresponding author, researcher, E-mail: tianyukui@cssrc.com.cn.

consider the allowable stress of the ice plate as a bearing medium. The interaction between the offshore structure and the ice sheet is nearly identical to the quasi-static loading form of a cylinder vertically breaking through ice sheet underneath, underscoring the importance of the design ice load for a cylinder vertically breaking through ice sheet. Research in this area not only enhances the ice-breaking capabilities of an underwater structure but also provides vital insights for offshore structure design.

The theoretical investigation of the ice load on cylindrical structures has been the subject of rapid advancement, with the predominant research method entailing the establishment of a mechanical model for vertical loading and its subsequent solution through computer programming^[4]. Notably, Chuang^[3] suggests that the effect of water is of relatively minor significance in the vertical ice-breaking process of a cylinder. Utilizing the fundamental assumption of the small deflection theory of elastic thin plates and the theory of elastic mechanics, Chuang could compute the deflection of a four-sided supported rectangular ice plate when subjected to a concentrated force.

Limited experimental research has been conducted on measuring the ice load during the time when a cylinder vertically goes upward to ice sheet. However, the research about ice load for a cylinder vertically downward loading can be used as a reference. For instance, Masterson et al^[5] investigated the allowable stresses of ice as a safe load-bearing medium, which can help ensure that long-term creep deformation will not lead to submersion of the ice surface. Furthermore, Wang^[6] conducted vertical ice-breaking tests on cylinders in an anhydrous environment using freshwater model ice on a self-developed test platform. The ice load of the cylinder was obtained through the observation of the destruction of the ice sheet during vertical ice-breaking process.

There have been several numerical simulation studies on ice load for a cylinder vertically breaking through ice sheet. A study by Ye et al^[7-8] employed the peridynamic method to develop a model of cylinder ice-breaking. The model was used to simulate the breakage process of sea ice and calculate the dynamic ice load on the cylinder. Meng^[9] established a numerical model of the action of underwater vehicle and ice plate using ANSYS/LS-DYNA. The model's effectiveness was verified by comparing it with the real ice-breaking process of the underwater vehicle. Additionally, Qian^[2] utilized the finite element method to investigate the dynamic characteristics of the ice load during the vertical upgoing of the underwater vehicle.

This paper aims to enhance the level of research on the ice load on underwater vehicles when passing from underneath ice covers using both model test and numerical simulation. The paper presents the observation of the destruction phenomenon of the ice sheet due to vertical loading, measurement of the overall ice load through a load sensor, and exploration of the measurement method of a cylinder vertically breaking through model ice sheet. The finite element method is employed to establish a numerical model for vertical loading on cylinders, which is compared with the model test results to verify numerical accuracy. Cylinder vertical loading simulations under various ice thicknesses and upgoing velocities are carried out, and the influences of different factors on the ice load of cylinders are analyzed. The study provides significant insights into the vehicle under vertical loading and structural design. It is anticipated that the results of this study will be of valuable reference to professionals in the field and will contribute to the development of effective solutions to the challenge of vertical ice-breaking.

1 Physical experiments

1.1 The columnar saline model ice

The Small Ice Model Basin of China Ship Scientific Research Center (CSSRC SIMB) has a dimension

of 8 m in length, 2 m in width, and 1 m in depth, as shown in Fig. 1^[10]. The ice-making process in the SIMB is similar to, but improved from, the method by the Evers^[11-12] of the Hamburg Tank (HSVA) in Germany. Cooling fans are suspended from the roof, ceiling panels with tiny holes are installed underneath to exhaust the cooling air, and circulating fans with guide plates are set on the side walls to suck the air used for cooling; thus, forced cooling air circulation is formed.



Fig.1 Interior scene of CSSRC SIMB

Model ice is made of sodium chloride solution, and the preparation process is divided into precooling, crystallization and ice making. To control the density and to lower the strength, an underwater air bubbling system is used to produce air bubbles which will be trapped in the model ice during the freezing process. Its mechanical properties can be adjusted by warming up and underwater air bubble generation system. After warming up, the temperature of model ice is usually around $-0.8\text{ }^{\circ}\text{C}$.

The mechanical properties of model ice in the SIMB are statistically analyzed through a series of experimental measurements. The main characteristic parameters of model ice ($-0.8\text{ }^{\circ}\text{C}$) in the SIMB and sea ice are summarized in Tab. 1. With the continuous exploration of the experimenters, it is found that after adding bubbles to the saline model ice, the brittleness of the ice is greatly improved. The flexural fracture mode of the ice and the distribution ratio of the crushed ice flakes of various scales are consistent with those of natural sea ice, and the similarity could be maintained in terms of physical and mechanical properties and fracture behavior patterns^[13].

Tab.1 Physical and mechanical parameters of sea ice and model ice in SIMB

Parameter/Unit	One-year columnar sea ice	Model ice
Density/($\text{g}\cdot\text{cm}^{-3}$)	0.91(average)	0.9–0.92
Thickness/mm	500–2000	30–50
Flexural strength/MPa	0.5–2	0.03–0.1
Compressive strength/MPa	0.5–12	0.05–0.2
Tensile strength/MPa	0.2–0.8	0.01–0.03
Elastic modulus/GPa	2–5	0.06–0.2

The model ice comprises a granular structure of fine particles, with a transitional sheet in the middle and a columnar structure at the lower sheet^[10]. As illustrated in Fig. 2(a), the crystal structure of the model ice is discernible. The crystal structure of the model ice is found to be very similar to that of the Arctic sea ice. In Fig. 2(b)^[14], Sta1, Sta2, Sta5, and Sta6 represent the Arctic one-year ice, while Sta3 represents the two-year ice and Sta4 represents the multi-year ice. The results indicate that the crystal structure of the model ice is similar to that of the Arctic one-year ice. Additionally, photographic and image analysis techniques are employed to obtain the crystal structure of the ice surface, which can be observed in Fig. 3.

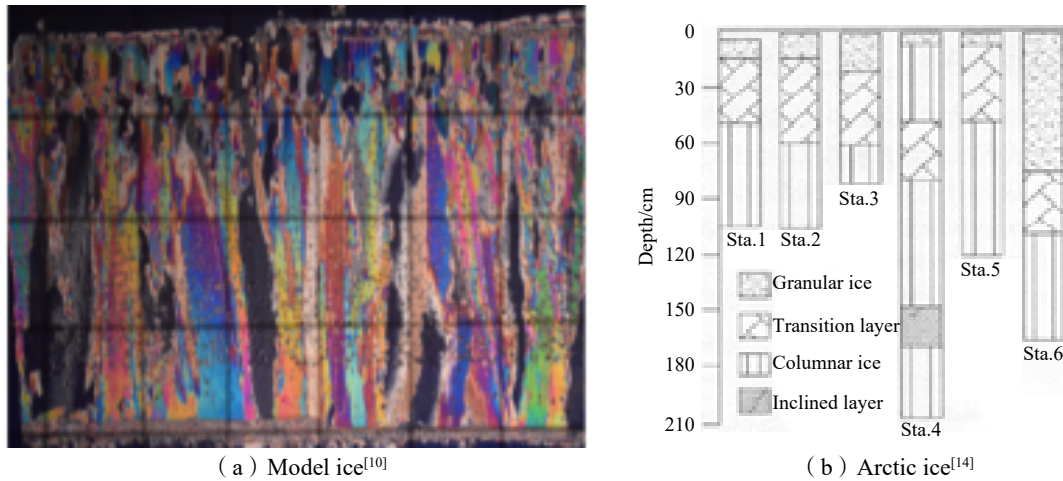


Fig.2 Ice crystal structure (Vertical slice)

1.2 Cylinder vertical loading test

The experimental model utilizes a cylindrical structure with a diameter of 30 mm and a height of 110 mm. A cylindrical mounting platform is provided, centered with an internal threaded hole. One end of the load cell is connected to the model via a screw rod, while the other is connected to the upper device. The load cell has a maximum capacity of 500 N. The main component of the power device is an air pump loading device, vertically installed on a square base. The loading speed is fixed at 25 mm/s. For visual reference, it is shown in Fig. 4 for the complete setup of the test device.



Fig.3 Model ice crystal structure (Horizontal slice)^[10]

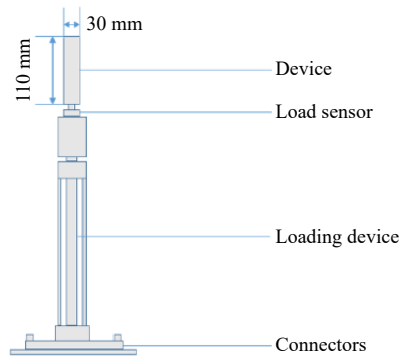


Fig.4 Test device

The vertical loading process is observed using a high-speed camera system to monitor the destruction of the ice sheet. The load sensor is used to obtain the overall ice load on the cylinder's upper surface, and the cylinder's subsequent changes in the ice load are analyzed. Tab. 2 displays the relevant instrumentation parameters of the test, while Tab. 3 outlines the specific test conditions.

Tab.2 Instrument specifications for cylinder vertical loading test

Instrument	Function	Range/Accuracy
Salinity meter	Measure the salinity of the ice	0.01 ppt
Electronic scales	Measure the density of ice	0.1 g
Vernier calipers	Measure the thickness of the ice sample	0.05 mm
High-speed cameras	Capture the details of the ice breakdown failure	2800 FPS
Load sensor	Measure the ice load	500 N
Air pump loading device	Control the speed of the cylinder	25 mm/s

Tab.3 Cylinder vertical loading test parameters

Case	Ice thickness/mm	Ice length/mm	Ice width/mm	Speed/(mm·s ⁻¹)
1	30	5000	2000	25
2	30	4000	2000	25
3	30	3000	2000	25

The test process mainly includes preparation of model ice, calibration of the load cell, installation of the cylinder and the load cell, measurement of the basic physical and mechanical properties of the model ice, and measurement of the ice load. The model ice is shown in Fig. 5. Adjacent to the basin, a high-speed camera is positioned and adjusted for optimal angle and focus. Three upgoing tests are carried out, with the ice load being recorded during each of these tests. Simultaneously, the ice surface rupture is observed via cameras and high-speed cameras.



Fig.5 Test initial state—model ice sheet

1.3 Experiment phenomenon

To facilitate the description of the test process, the photos of the three stages of the cylinder moving, the destruction of the ice sheet, and the breakthrough of the cylinder are mainly listed, as shown in Figs. 6–8.



Fig.6 First test (ice length 5000 mm, ice width 2000 mm)



Fig.7 Second test (ice length 4000 mm, ice width 2000 mm)

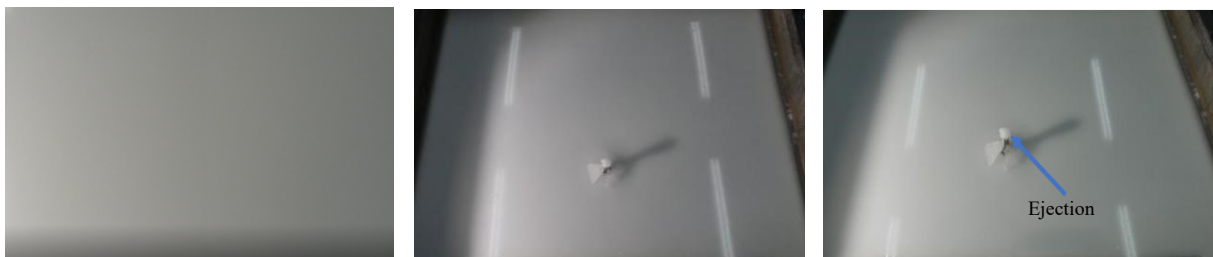


Fig.8 Third test (ice length 3000 mm, ice width 2000 mm)

As per the test process, when a cylinder breaks the ice vertically, it initiates a radial crack around the cylinder that extends toward both ends. Following this, a second crack appears perpendicular to the first crack and extends towards both ends until it reaches the vicinity of the ice plate. The fan-shaped ice sheet around the cylinder also undergoes warping, leading to the ejection of a portion of the ice sheet. Additionally, a circumferential crack originates from the ice-breaking position of the cylinder at the end of the radial crack. Notably, the destruction of the ice sheet observed during the test aligns with the cylindrical loading test of sea ice carried out by Sodhi^[15]. When the ratio of the diameter of the indenter to the thickness of the ice sheet is less than 2, the failure of the ice sheet is mainly shear. To further analyze the destruction of ice, the high-speed camera photographs are given in Fig. 9. As can be seen from Fig. 9, the columnar sheet of the ice sheet directly above the cylinder is clearly separated from the granular sheet. For this test, it can be assumed that the ice sheet has undergone shear failure.

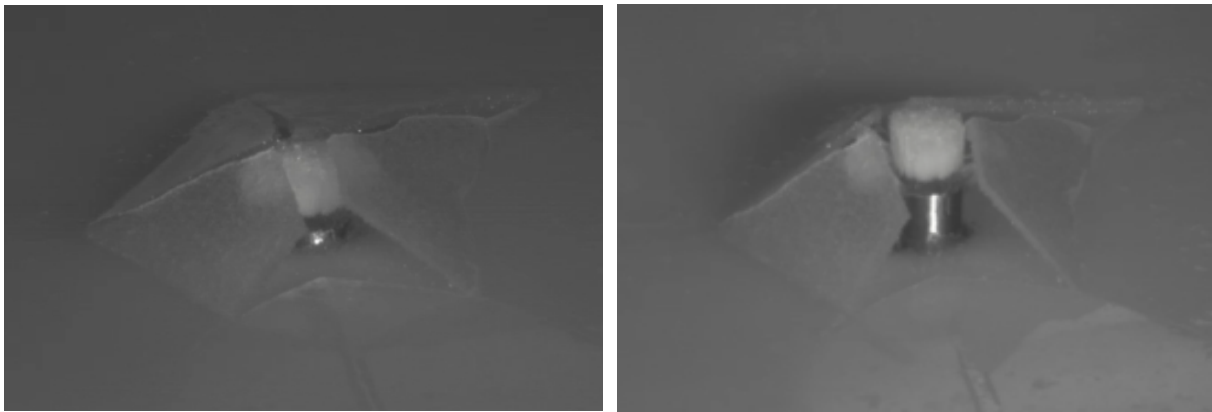


Fig.9 High-speed camera results

In this section, the high-frequency sampling data collected from three ice-breaking tests are filtered to obtain the loads, as illustrated in Fig. 10. It is demonstrated that the extreme values of the ice load in the vertical loading tests do not change significantly, and the difference is within 15%, thereby underscoring the robustness of the results. Consequently, the length variation of the ice sheet ranging from 3–5 m has slight effects on the test results.

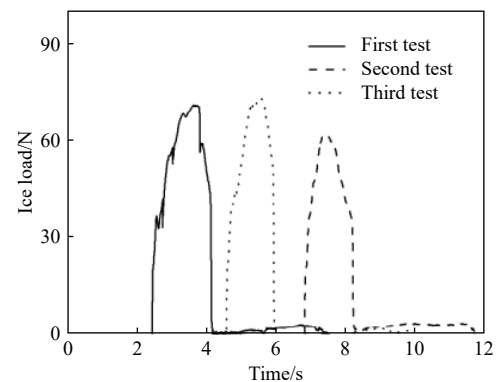


Fig.10 Ice load data of three tests

2 Numerical modeling

2.1 Numerical model of ice material

A big advantage of the finite element method is that many contact algorithms allow the coupling of ice and structural models. Therefore, in this paper, the finite element solver LS-DYNA is used to establish a model ice failure model. The calculation method used by the nonlinear finite element program is the explicit integration method^[16].

When using the finite element method to simulate the model ice mechanical test, it is necessary to determine the material model parameters that match the macroscopic characteristics of the material. Standard

ice constitutive models include the elastoplastic model, elastic brittleness model, etc.. According to Karr and Choi^[17], model ice materials are considered isotropic in their undeformed state. This assumption is adopted in this paper, so the isotropic elastoplastic fracture model (*MAT_ISOTROPIC_ELASTIC_FAILURE) in LS-DYNA is selected to simulate the model ice. The failure criterion for the material is the Von Mises yield criterion.

The material parameters of the model ice are shown in Tab.4. The specific parameters of density, plastic hardening modulus and plastic failure strain are obtained by the model ice mechanical test. According to the relevant ice numerical simulation^[18], the ranges of other material parameters are obtained, and the specific parameters are given in Tab.4.

Tab.4 Model ice material parameters

Material properties	Value	Material properties	Value
Density/(g·cm ⁻³)	0.92	Bulk modulus/MPa	75
Shear modulus /MPa	76.9	Plastic failure strain	0.05
Plastic hardening modulus /MPa	94.7	Failure pressure/kPa	-110
Yield stress/kPa	83		

According to von Bock und Polach^[19], the air pore inside the model ice can be simulated by deleting elements using a random algorithm, and the number of deleted elements depends on the porosity. This is another advantage of numerical simulation compared with the experiments in Chapter 1 because ice porosity is difficult to control according to pre-determined values. The K file of the model ice numerical model is employed, and the random number function is set to delete a part of the model ice elements according to the input value of porosity, as shown in Fig. 11.

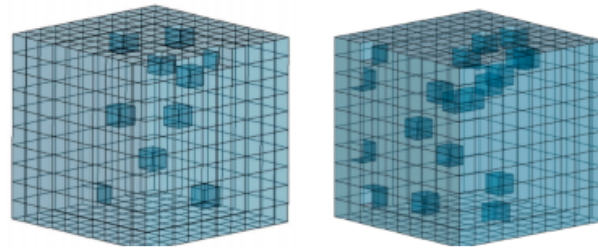


Fig.11 Ice with internal defects^[20]

2.2 Numerical simulation of cylinder vertical loading test

A numerical simulation of a cylinder vertical loading test is to be conducted based on the prior research. The primary focus of this paper is the ice load on the cylinder. Therefore, only the cylinder's appearance and shape need to be considered. A rigid body is selected as the material model for the cylinder. The geometric dimensions of the ice sheet are the same as those in the basin, and the specific parameters are shown in Tab.3.

Solid elements are selected for the ice and cylinder types. To ensure that the calculation results are accurate enough, the number of elements and nodes in the meshing of the model ice body is large, but the number of elements has a great influence on the calculation time. Based on the above reasons, the mesh convergence of the model is analysed by flexural strength test simulation. Four grids with different element sizes are selected, which are 0.5 cm × 10 cm × 4 cm, 0.5 cm × 5 cm × 2 cm, 0.5 cm × 2.5 cm × 1 cm, and 0.5 cm × 1.25 cm × 0.5 cm, respectively. Then the calculation results of the mesh division with different element sizes are compared and analyzed. As can be seen from Fig. 12, the difference between the calculation

results obtained by the model ice simulation with element size of $0.5\text{ cm} \times 10\text{ cm} \times 4\text{ cm}$ and with the size of $0.5\text{ cm} \times 1.25\text{ cm} \times 0.5\text{ cm}$ is only 7%, which indicates that the convergence of the grid is very good. Considering the computing efficiency, the initial meshing element size is selected as $0.5\text{ cm} \times 5\text{ cm} \times 2\text{ cm}$. To improve the accuracy of the calculation results, dense gridding is performed on the ice near the cylinder, as shown in Fig. 13.

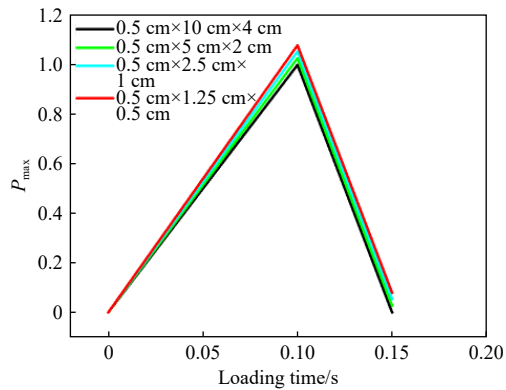


Fig.12 Grid convergence analysis

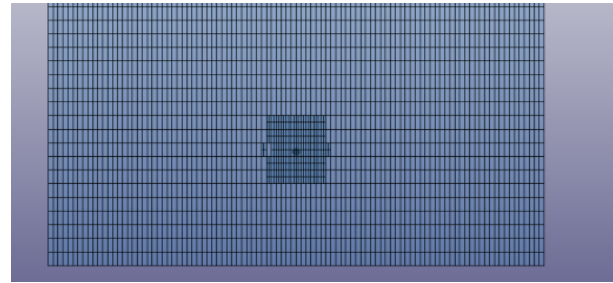


Fig.13 Meshing of numerical models

Considering the verification work in this paper, the numerical model adopts the boundary condition of fixed support on three sides and free on one side. The degrees of freedom of the cylinder are the same under the three test conditions. Only the degrees of freedom in the Z direction and the speed of the upward movement are the same, and the speed is 2.5 cm/s . Refer to previous work^[20] for the internal defects of the ice structure under three conditions, the bubble volume of the ice sheet is 1.5%.

2.3 Time history curve and failure mode of model ice

The test results and the numerical simulation results are compared from two aspects of the time history curve and failure phenomenon.

The comparison about time history curve is presented in Fig. 14. During the vertical loading process of the cylinder, the peak forces of the time history curves of the physical test and numerical simulation are relatively similar. However, the changing patterns of the time history curve differ because of the structural differences between the actual model ice and the numerical model. The actual model ice structure comprises a granular sheet and a columnar sheet, whereas the numerical model is a single isotropic material with different material properties.

Upon the cylinder upgoing, the ice load changes more gently in the rising stage of the time history curve due to the deflection and crack produced by the granular sheet on the ice surface of the actual model. The columnar sheet underneath is separated from the surrounding ice sheet and pushed up the granular sheet. In contrast, the numerical model is an isotropic material, and the material properties of the two are different, so the numerical model's time history curve is more rapid in the rising stage. In addition, the influence of the fluid under the ice sheet is not considered in the numerical simulation, so the unloading curve is very different from the actual curve after the model ice

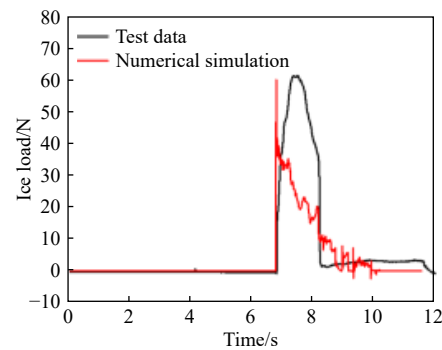


Fig.14 Comparison of ice load between numerical simulation and mechanistic test

failure. Even though there is such a difference between the two curves, it does not affect the extreme value of the ice load. Thus, the rationality of the ice simulation model can be verified from the peak values of the time history curves.

A comparison between the numerical simulation of ice failure and the model ice failure captured by a high-speed camera is illustrated in Fig. 15. The results indicate that the ice sheet around the cylinder warps, and cracks appear when subjected to vertical loading. This observation further confirms the rationality of the ice simulation model through the comparison of failure phenomena.

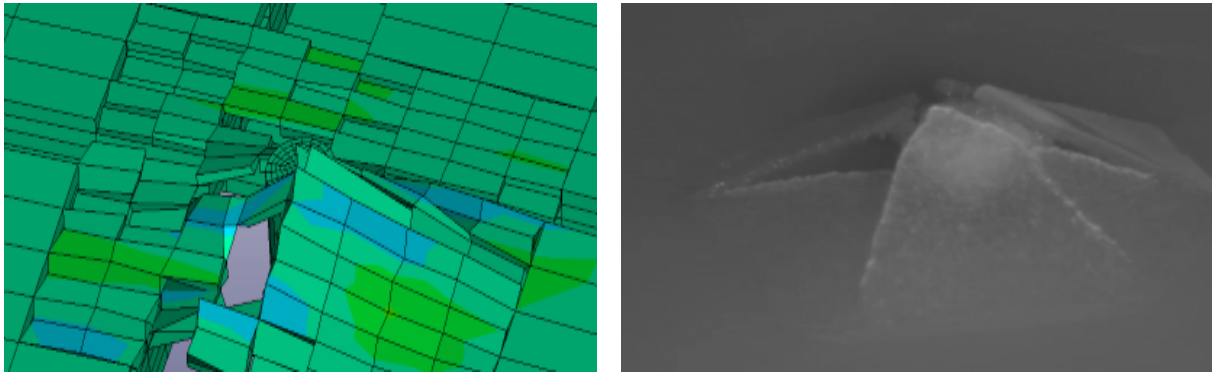


Fig.15 Comparison of numerical simulation with a mechanistic test on the failure phenomenon

2.4 Effect of ice sheet thickness

Fig. 16 displays the variation of ice failure concerning ice thickness at a constant upgoing speed of 30 mm/s. The results indicate that an increased ice thickness leads to an increased crack area. While the degree of warping of the ice sheet decreases with ice thickness increasing, the extrusion gradually increases, resulting in more failure units and a larger crack area in the ice sheet. Hence, thicker ice leads to a higher ice load on the cylinder to break through the ice vertically. This correlation highlights the calculation results from a macroscopic viewpoint and verifies the numerical calculation results' reliability.

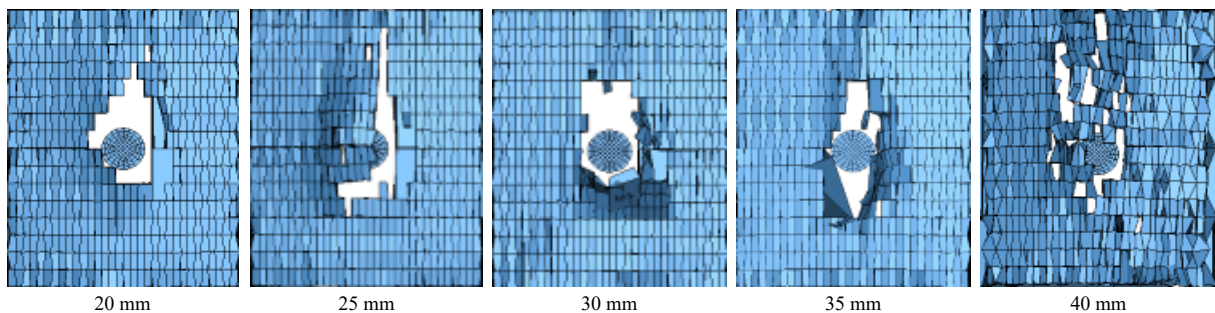


Fig.16 Effect of ice thickness on ice sheet destruction

Diverse seasons and regions exhibit variations in sea ice thickness, which significantly impact the ice load of the cylinder. Thus, the influence of ice thickness on the ice load of the cylinder based on numerical results is examined in this section. Fig. 17 depicts the ice load's fluctuation with ice thickness at a constant upgoing speed of 30 mm/s. As illustrated in the figure, despite the fluctuation of individual points (35 mm), the cylinder's ice load surges with the increase in ice thickness. Therefore, a thinner ice sheet area should be preferable for ice-breaking operations.

From the above two diagrams, it can be concluded that in the range of 20–40 mm, the thicker the ice is, the greater the icebreaking load required, and the larger the ice destruction area is.

2.5 Effect of upgoing speed

The effect of upgoing speed on ice failure under an identical ice thickness of 25 mm is studied in this section, and the findings are presented in Fig. 18. The ice sheet undergoes noticeable warping, and there is an accumulation of broken ice around the cylinder. In this velocity range, the velocity change has a certain effect on the damage area. When the velocity is 20 mm/s, the damage area is the biggest, and at 30 mm/s the ice sheet flips more violently. This indicates that when the speed is slow, more time is given for the crack to grow fully; and when the speed increases, the cylinder directly pushes out of the ice, while the crack propagation is not timely.

The upgoing speed of the cylinder is a critical factor in the operation of the cylinder. Consequently, the influence of the cylinder's upgoing speed on the ice load based on numerical results is examined in this section. Fig. 19 illustrates that as the upgoing speed of the cylinder increases, the ice load of the cylinder undergoes slight changes. When the velocity is 20 mm/s, the loading on the cylinder is closer to the quasi-static loading, the deflection of the ice plate changes more calmly, and some cracks are generated which reduces the peak force of the ice load during failure. Nevertheless, the variation range is minimal, and the strength difference of the ice load under different upgoing speeds is within 15%. Hence, based on Fig. 19, it can be inferred that the cylinder's upgoing speed does not have a quite significant effect on the ice load when it is between 20 mm/s and 30 mm/s.

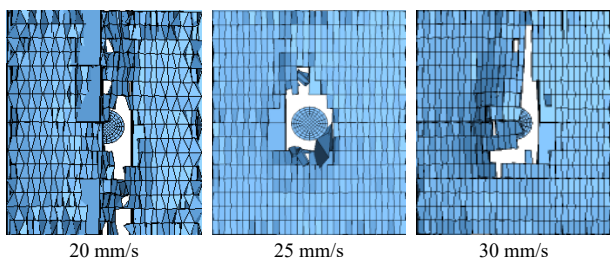


Fig.18 Effect of upgoing speed on ice sheet destruction

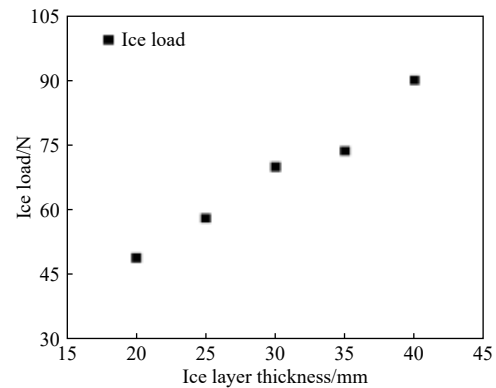


Fig.17 Effect of ice thickness on ice load

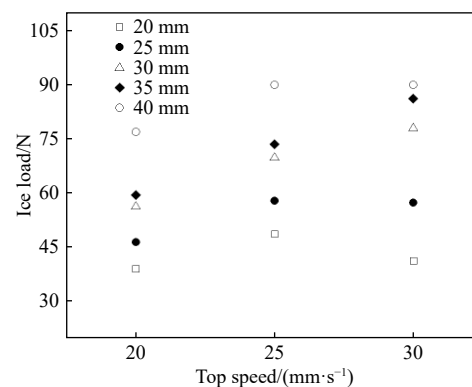


Fig.19 Effect of upgoing speed on ice load

3 Conclusions

In this paper, physical experiments and numerical modeling are carried out to investigate the cylinder vertical ice-breaking load from a columnar saline model ice sheet. The influence of different factors on the ice-breaking load of model ice is analyzed, and the crack propagation law of the ice sheet is found out. The main conclusions are as follows:

(1) When the cylinder breaks the ice sheet upwards at a constant loading speed, the ice plate above the cylinder warps, and then the ice surface is broken. Local radial cracks are generated around it, and with the cylindrical icebreaking position as the circle's center, hoop cracks appear, and some radial cracks continue to

extend until they go near the free end of the ice. In addition, the columnar sheet of the ice sheet directly above the cylinder is clearly separated from the granular sheet.

(2) The extreme value of the ice load in the three tests is relatively close, and the difference is controlled within 15%. Therefore, it can be considered that when a cylinder with a diameter of 30 mm breaks the ice sheet upwards, the model ice sheet with a length of 3~5 m has slight effects on the test results. The cylinder's ice load surges with the increase of ice thickness, but as the upgoing speed increases, the ice load undergoes slight changes. The velocity change has a certain effect on the damage area. When the speed is slow, more time is given for the crack to grow fully; and when the speed increases, the cylinder directly pushes out of the ice, and the crack propagation is not timely.

The study of the vertical ice-breaking ice load of the cylinder provides a feasible means for the prediction of the vertical ice-breaking ice load and a reliable reference for the structural reinforcement design and safety assessment of structures in the ice area.

References

- [1] Guan L, Yan B, Wang N. Spatio-temporal pattern of China-Europe arctic vehicleping routes and seaworthy vehicle[J]. *Navigation of China*, 2018, 41(2): 124–129.
- [2] Qian Y. Study on the calculation method for the ice-load of vertical ice-breaking[D]. Harbin: Harbin Engineering University, 2020.
- [3] Chuang J S. Experimental study and numerical analysis of vertical ice breaking[D]. Harbin: Harbin Engineering University, 2021.
- [4] Yue J Z, Wu X Q, Huang C G. Multi-field coupling effect and similarity law of floating ice break by vehicle launched underwater[J]. *Chinese Journal of Theoretical and Applied Mechanics*, 2021, 53(7): 1930–1939.
- [5] Masterson D M. State of the art of ice bearing capacity and ice construction[J]. *Cold Regions Science and Technology*, 2009, 58(3): 99–112.
- [6] Wang C, Wang J, Wang C. Research on movement of cylindrical structure out of water and breaking through ice sheet based on S-ALE method[J]. *Chinese Journal of Theoretical and Applied Mechanics*, 2021, 53: 3110–3123.
- [7] Ye L Y, Guo C Y, Wang C, et al. Peridynamic solution for submarine surfacing through ice[J]. *Vehicles and Offshore Structures*, 2020, 15(5): 535–549.
- [8] Ye L Y, Wang C, Guo C Y, et al. Peridynamic model for submarine surfacing through ice[J]. *Chinese Journal of Vehicle Research*, 2018, 13(2): 51–59.
- [9] Meng X B. Research on the force of submarine to destroy the ice sheet upwards[D]. Harbin: Harbin Institute of Technology, 2019.
- [10] Tian, Y K, Ji S P, Wang Y H, et al. Research on sea ice simulation and measurement in small ice model basin of CSSRC[J]. *Marine Environmental Science*, 2021, 40(2): 277–286.
- [11] Evers K U. Model tests with vehicles and offshore structures in HSVA's ice tanks[C]//*Proceedings of the POAC'2017*. Busan Korea: Port and Ocean Engineering under Arctic Conditions (POAC), 2017.
- [12] Evers K U, Jochmann P. An advanced technique to improve the physical properties of model ice developed at the HSVA ice tank[C]//*Proceedings of the POAC '93*. Hamburg, Germany: Port and Ocean Engineering under Arctic Conditions (POAC), 1993: 877–888.
- [13] Yu C G. Research on ice loading of typical offshore ice-resistant structure[D] Wuxi: China ship Scientific Research Center, Wuxi, 2021.
- [14] Han H W. Study on the spatial and temporal distribution of sea ice and the physical, mechanical properties of sea ice in polar routes[D]. Dalian: Dalian University of Technology, 2016.
- [15] Sodhi D S. Breakthrough loads of floating ice sheets[J]. *Journal of Cold Regions Engineering*, 1995, 9(1): 4–22.

- [16] Guo T, Zhang A, Yu B. Underwater collision simulation of the pressure hull with spherical head based on LS-DYNA[J]. J. Vehicle Mech., 2021, 25: 210–219.
- [17] Karr D, Choi K. A 3-dimensional constitutive failure model for polycrystalline ice[J]. Mech. Mater, 1989, 8: 55–66.
- [18] Zhao W, Tian Y, Yu C. Experimental investigation on breaking strength of model ice with circular ice plate indentation tests[C]//Proceedings of the 32nd International Ocean and Polar Engineering Conference, Shanghai, China, 2022.
- [19] Rüdiger Von Bock und Polach R B, Ehlers S. Model scale ice-Part B: Numerical mode[J]. Cold Reg. Sci. Technol, 2013, 94: 53–60.
- [20] Tian Y, Zhao W, Yu C, et al. Investigations on flexural strength of a columnar saline model ice under circular plate central loading[J]. Water, 2023, 15(19): 3371.

水下垂向作用于模型冰层的圆柱体冰载荷研究

赵伟航, 田于逵, 季少鹏, 刚旭皓, 余朝歌, 孔 帅

(中国船舶科学研究中心, 江苏 无锡 214082)

摘要: 水下航行器从冰盖下方顶出冰层过程中所承受的冰载荷, 是极地工程领域重点关注的问题。目前国内对此问题的研究尚不成熟, 无论是机理性试验测量还是数值模拟计算都存在许多难点需要克服。本文以柱体水下垂向顶冰冰载荷为研究主题, 在中国船舶科学研究中心小型冰水池内开展柱体顶冰机理性试验研究, 采用高速摄像系统观测柱体顶冰过程中冰层破坏现象, 可见以圆柱体破冰位置为圆心, 产生局部的径向裂纹和环向裂纹。与此同时, 使用有限元软件 LS-DYNA 对这一过程进行数值模拟, 研究分析冰厚和上浮速度对冰载荷的影响。对不同工况下的计算结果进行统计分析, 确定各因素对冰载荷的影响。本研究探索了柱体水下垂向顶冰的试验测量方法, 测试结论可为冰区作业的水下航行器结构强度设计提供参考。

关键词: 圆柱体; 模型试验; 破坏模式; 裂纹扩展; 冰载荷; 数值模拟

中图分类号: P75 P731.15 **文献标识码:** A

基金项目: 国家自然科学基金资助项目(52192694; 52192690); 高技术船舶科研项目([2021]342号)

作者简介: 赵伟航(1998–), 男, 中国船舶科学研究中心助理工程师;

田于逵(1968–), 男, 中国船舶科学研究中心研究员。